


RESEARCH ARTICLE

Unconventional mRNA processing and degradation pathways for the polycistronic *yrzI* (*spyTA*) mRNA in *Bacillus subtilis*

Laetitia Gilet¹, Magali Leroy¹, Alexandre Maes², Ciarán Condon¹ and Frédérique Braun¹ ¹ Expression Génétique Microbienne, CNRS - Université Paris Cité, Institut de Biologie Physico-Chimique, Paris, France² Plateforme de Génomique Fonctionnel, UMR8226 CNRS Sorbonne Université, Institut de Biologie Physico-Chimique, Paris, France**Correspondence**

F. Braun and C. Condon, Expression Génétique Microbienne, CNRS - Université Paris Cité, Institut de Biologie Physico-Chimique, 13 rue Pierre et Marie Curie, 75005 Paris, France
Tel: +33 1 58 41 51 23
E-mail: braun@ibpc.fr, condon@ibpc.fr

Laetitia Gilet and Magali Leroy contributed equally and are listed alphabetically

(Received 19 November 2024, revised 7 February 2025, accepted 10 February 2025, available online 8 March 2025)

doi:10.1002/1873-3468.70027

Edited by Christian Griesinger

The ribosome-associated endoribonuclease Rael cleaves the *Bacillus subtilis* *yrzI* operon mRNA in a translation-dependent manner. This operon encodes up to four small peptides, S1027, YrzI, S1025, and S1024, whose functions are unknown. Here, we identified the function of YrzI and S1025 and deciphered the degradation pathways of the *yrzI* polycistronic mRNA. We show that YrzI is toxic at high concentrations, but co-expression with S1025 abolishes its toxicity, and that, in the absence of Rael, S1025 is the major antidote to the YrzI toxin. We show that a highly stable mRNA species containing the YrzI and S1025 open reading frames results from endoribonucleolytic cleavage upstream of *yrzI* followed by the arrest of 5'-exoribonucleolytic processing by ribosomes bound to its exceptionally strong Shine-Dalgarno sequence. Degradation of this mRNA requires either translation-dependent cleavage within S1025 by Rael or direct attack from the structured 3'-end by 3'-exoribonucleases. Neither pathway is common for a *B. subtilis* mRNA.

Keywords: *B. subtilis*; Rael; RNA maturation and decay; RNases; translation

Two major mRNA degradation pathways have been characterized in *Bacillus subtilis* thus far [1,2]. The 5'-exoribonucleolytic (5'-exo) pathway resembles the mRNA decapping and Xrn1-dependent pathway found in eukaryotes [1,2]. After deprotection of the mRNA by an RNA pyrophosphohydrolase, e.g., BsRppH, the 5'-exoribonuclease complex RNase J1/J2 degrades the mRNA all the way to the 3' end [3]. In the endoribonucleolytic (endo) pathway, the mRNA is cleaved internally and the resulting fragments degraded by either 3'- or 5'-exoribonucleases. The key endoribonucleases known to initiate mRNA decay in *B. subtilis* are the single strand-specific enzyme RNase Y, a functional analog of *E. coli* RNase E, and the double strand-specific

enzyme RNase III [4]. In general, the activity of these enzymes is inhibited by translation, with the flow of ribosomes occluding access to cleavage sites within open reading frames (ORFs) [5–9]. In 2017, we identified a novel component of the *B. subtilis* mRNA decay machinery, the ribosome-associated endoribonuclease Rael [10] that, in contrast to RNase III and RNase Y, requires translation for cleavage [11,12].

We have thus far identified two Rael targets: the *bmrBCD* operon mRNA [12], encoding a multidrug transporter, and the *yrzI* operon mRNA [10]. Ribosome profiling experiments have suggested that the latter operon, in addition to encoding the annotated 49-amino acid (aa) YrzI peptide, expresses

Abbreviations

aa, amino acid; nt, nucleotide; ORF, open reading frame; SD, Shine-Dalgarno; spyA, small peptide yrzI antitoxin; spyT, small peptide yrzI toxin; TA, toxin-antitoxin.

three supplementary peptides S1027, S1025 and S1024, that are 38, 17, and 52 aa's in length, respectively [13]. We previously showed that RaeI cleaves within the S1025 ORF in a translation-dependent manner, confirming that the 17-aa S1025 peptide is indeed translated [10]. However, the functions of the different peptides expressed from this operon remain mysterious.

Here, we show that the overexpression of the YrzI peptide impairs *B. subtilis* growth, an effect that is counteracted by S1025, suggesting that these two peptides constitute a toxin-antitoxin (TA) system. We also show that expression of this operon is governed at the transcriptional level by the transition state regulator, AbrB, and at the post-transcriptional level via non-canonical mRNA processing and degradation pathways. Two primary transcripts undergo processing to a short highly stable ~ 500 nt mRNA fragment that is protected from 5'-degradation by ribosomes bound to an exceptionally strong Shine-Dalgarno (SD) sequence located upstream of *yrzI*. With the 5'-degradation pathway blocked by initiating ribosomes, elimination of this mRNA fragment requires degradation by one of two alternative pathways (i) translation-dependent endoribonucleolytic cleavage by RaeI, followed by degradation of the unprotected upstream and downstream fragments by 3'- and 5'-exoribonucleases or (ii) direct attack by 3'-exoribonucleases from the 3' end of the mRNA despite the presence of a protective transcription terminator.

Materials and methods

Strain construction

Oligonucleotides and strains used in the paper are listed in Tables S1 and S2, respectively.

The *rph::spc*, *rnr::tc*, *yhaM::pm*, *pnp::kan* and *pnp::cm* cassettes to make strains CCB329, CCB395, CCB396, CCB407, CCB409 and CCB1210 in our lab background (SSB1002 = W168 *trpC*+) were a kind gift from David Bechhofer, and have been described previously [14]. Strain CC376 was constructed by transferring the *raeI::pMUTIN* construct from strain CCB375 into CCB396. Strain CC761 was constructed by transferring the *rny::spec* construct from strain CCB441 into CCB375.

The plasmid overexpressing the YrzI peptide was constructed by amplifying the *yrzI* gene by PCR using oligos CC1731/1732 and cloned in pDG148 cleaved with SalI and HindIII. The resulting plasmid pDGYrzI (pl. 687) contains the *yrzI* gene under *Pspac* control, followed by an *E. coli* rRNA transcription terminator to limit transcription of downstream plasmid DNA. This plasmid was transformed into CCB375 (*AraeI*) to create strain CCB815. We initially failed to transform this plasmid into wild-type cells. We

thus re-isolated it from strain CCB815, transformed it with high efficiency into SSB1002 (WT) to create strain CCB839. The plasmid was re-isolated from CCB839 to confirm its sequence. pDGYrzI-S1025 (pl. 726) and pDGS1025 (pl. 727) were constructed by amplifying *yrzI*-S1025 and S1025 fragments by PCR using oligo pairs CC1731/1809 and CC1808/1809. PCR fragments were cleaved with SalI and HindIII and cloned in pDG148. The resulting plasmids were transferred to *B. subtilis* WT and *AraeI* cells to create strains CCB913, CCB914 (pl. 726) and CCB915, CCB916 (pl. 727), respectively.

Northern blots and primer extension assays

Northern blots were performed on total RNAs isolated either by the glass beads/phenol method described in [15] or by the RNAsnap method described in [16]. Northern blots were performed as described previously [4]. Primer extension assays were performed using the oligo CC1589 on glass bead/phenol extracted RNAs as described previously [17].

Spot dilution assays

Cells were grown in 2xYT medium to OD₆₀₀ = 0.6. When cells contained either the empty plasmid pDGYrzI (pl687), pDGYrzI-S1025 (pl726) and pDGS1025 (pl727), serial dilutions were spot on LB plates containing kanamycin (5 µg·mL⁻¹) to maintain the plasmid. When indicated, IPTG at 100 µM to induce the expression of the inserted gene was added.

Ribosomal subunit (30S) protection assay

Five nanomoles of a 3'-labeled (p³²Cp) *yrzI* RNA was mixed with 500 nM *B. subtilis* 30S ribosomal subunits isolated from an RNase J1-depleted strain as described in [17] in 4 µL RNase J1 reaction buffer. The *yrzI* RNA was synthesized *in vitro* by T7 RNA polymerase using a Mega-ShortScript kit (Thermo Fischer Scientific, Waltham, MA, USA) from PCR fragments amplified from chromosomal DNA using oligo pair CC3176/CC3042 (CC3176 had an integrated T7 RNA polymerase promoter sequence). Subunits were allowed to bind for 10 min at 37 °C, followed by 10 min on ice. A total of 1.8 µg (1 µL) RNase J1 was added to start the reaction. Reactions were incubated at 25 °C for 10 min, stopped as above, and loaded directly onto 5% polyacrylamide denaturing gels.

Results

YrzI encodes a toxic peptide that is counteracted by S1025

The *yrzI* operon encodes two proteins (YrhF and YrhG) and four small peptides S1027, YrzI, S1025,

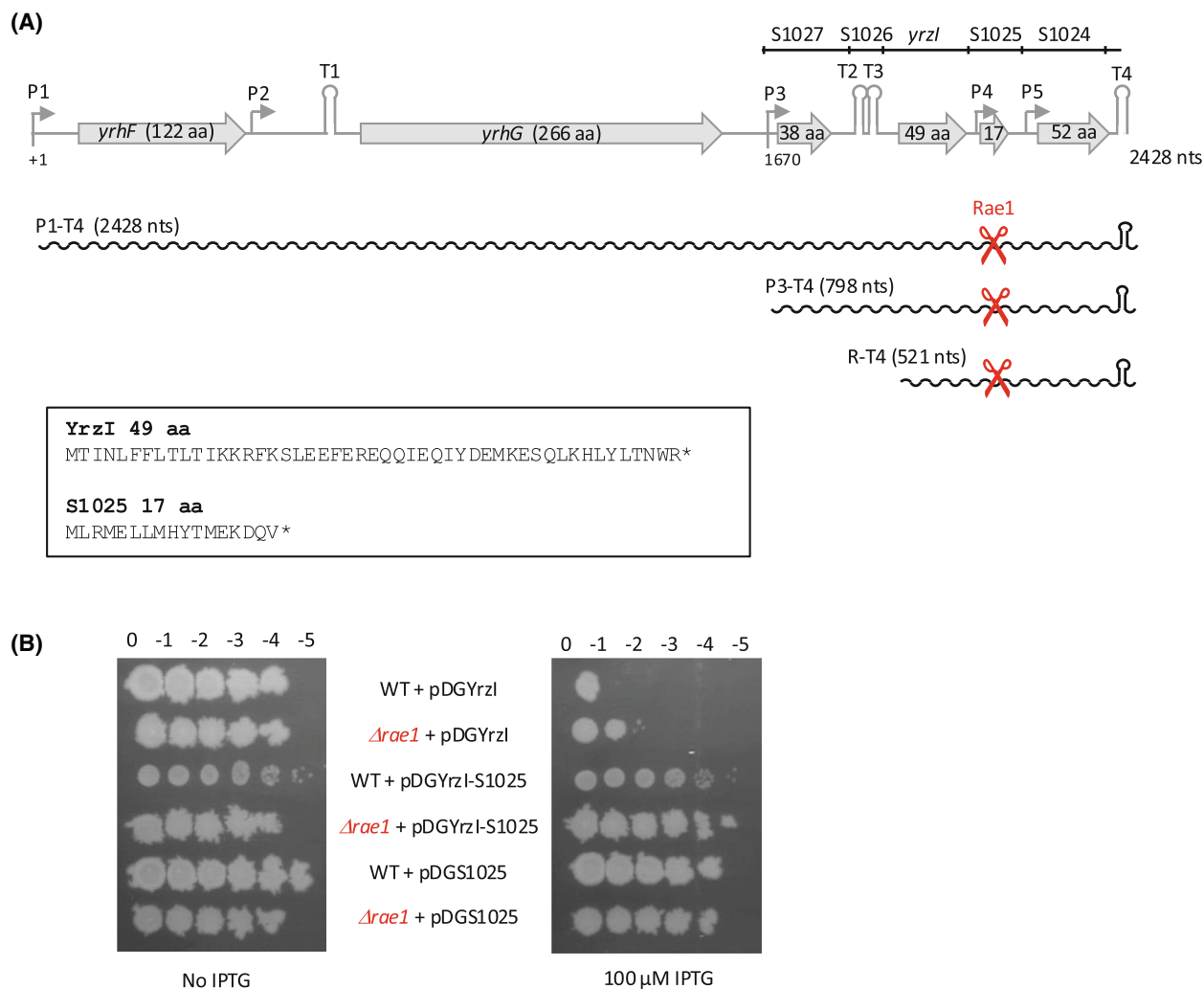


Fig. 1. The toxicity of YrzI is counteracted by S1025. (A) Structure of the *yrzI* operon. Putative ORFs are represented by gray arrows, the putative promoters by rightward-pointing arrows and putative transcription terminators by the hairpin structures and Rae1 cleavage site within *S1025* by scissors. The size of the ORFs is given in amino acids (aa). The transcripts from this locus are shown as wavy lines. The sequence of the YrzI and S1025 peptide is shown. (B) Ten-fold serial dilution of WT and *Δrae1* strains containing the YrzI, S1025 or YrzI+S1025 overexpression plasmids pDGYrzI, pDGS1025 and pDGYrzI-S1025, respectively, spotted on LB plates with or without IPTG (100 μM). This experiment was repeated three times.

and S1024, whose functions are all unknown (Fig. 1A). We previously showed that Rae1 cleaves within the *S1025* ORF in a translational-dependent manner between codons 13 and 14 to initiate the degradation of the *yrzI* polycistronic mRNA and that deletion of the *rae1* gene led to an accumulation of three major RNAs of ~ 2.4 kb (P1-T4), ~ 0.8 kb (P3-T4) and ~ 0.5 kb in size (R-T4), all containing the *yrzI* open reading frame [10] (Fig. 1A). Since small peptides can have toxic effects on bacterial cell growth [18], we wondered whether the Rae1 cleavage site within S1025 might serve to eliminate this mRNA to protect cells from potential toxicity of one of its encoded peptides.

Because YrzI was the originally annotated peptide of this operon and we had direct evidence that S1025 was translated, we began by analyzing the effect of these two peptides on cell growth by constructing two replicative plasmids, pDG-YrzI and pDG-S1025, permitting overexpression of YrzI and S1025 under control of an IPTG-dependent promoter. Induction of *yrzI* expression by addition of IPTG led to a 3- to 4-log inhibitory effect on *B. subtilis* growth in WT and *Δrae1* cells (Fig. 1B), suggesting that the YrzI peptide is indeed toxic at high doses. In contrast, no toxic effect of S1025 overexpression was observed in either WT or *Δrae1* cells (Fig. 1B). Since many toxins are encoded in

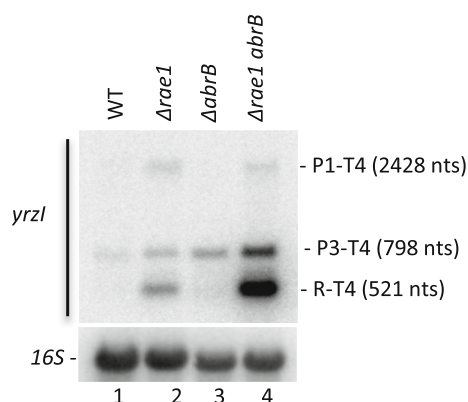


Fig. 2. The polycistronic *yrzI* mRNA is regulated by AbrB at the transcriptional level. Northern blot showing steady state level of the *yrzI* and *abrB* transcripts in WT, $\Delta rae1$, $\Delta abrB$ and $\Delta rae1 \Delta abrB$ strains at mid-log phase (OD₆₀₀ = 0.5). The blot was probed with oligo CC1589 (*yrzI*) and with a probe complementary to 16S rRNA (CC058) as a loading control. This experiment was repeated twice.

operons with their antitoxins just downstream [18], we assayed the effect of producing both peptides together by cloning the *YrzI* and *S1025* region under control of an IPTG-dependent promoter (pDG-*YrzI*-*S1025*). Remarkably, co-expression of *S1025* abolished the toxicity of *YrzI* (Fig. 1B). The protective effect of adding *S1025* is not simply due to destabilization of the *yrzI*-*S1025* mRNA through addition of the *Rae1* cleavage site, since expression of *S1025* neutralized the toxicity of *YrzI* even in absence of *Rae1* (Fig. 1B).

Thus, two different levels of controlling *YrzI* expression/toxicity exist: cleavage of its mRNA by *Rae1* within the *S1025* ORF and a *Rae1*-independent antitoxin effect of the *S1025* peptide.

The polycistronic *yrzI* mRNA is regulated by AbrB at the transcriptional level

It has previously been shown that the expression of the *bmrBCD* operon is repressed by the transition state regulator AbrB at the transcriptional level [19], in addition to the post-transcriptional regulation mediated by *Rae1* [12]. Interestingly, transcriptional repression by AbrB is also predicted to be shared by the *yrzI* operon [20] and an AbrB binding site was mapped upstream of the P3 promoter [21]. To confirm this, we measured the levels of *yrzI* mRNA in strains lacking *rae1*, *abrB* or both, at mid-exponential growth phase, by Northern blot (Fig. 2). Deletion of *abrB* alone caused a small accumulation of the P3-T4 *yrzI* transcript compared to WT (Fig. 2, compare lane 3 to 1), and deletion of both *rae1* and *abrB* caused greater increase in accumulation of both P3-T4 and R-T4

RNAs than deletion of *rae1* alone (Fig. 2, compare lane 4 to 2). These results confirm that AbrB is a repressor of *yrzI* operon expression in mid-exponential phase. Expression of the *yrzI* operon is thus modulated at two levels, transcriptionally by AbrB and post-transcriptionally by *Rae1*.

Mapping of the major RNAs produced from the *yrzI* locus

A transcriptome study by [22], identified several potential promoter (P1, P2, P3, P4, and P5) and terminator sequences (T2, T3, and T4) around the *yrzI* locus (Fig. 1A). However, Northern blots probed for *yrzI* only accounted for transcripts originating at P1 or P3 and ending at T4 (Fig. 3A, left panel). To get a more complete picture of the RNAs mapping to this locus, we hybridized Northern blots with oligonucleotide probes complementary to the *S1027* or *S1024* ORFs, upstream and downstream of *yrzI*, respectively. To determine their sensitivity to *Rae1*, these blots contained total RNA isolated from WT, $\Delta rae1$ and plasmid complemented strains grown in the absence or presence of IPTG.

As seen previously [10], only the 2.4 kb (P1-T4), 0.8 kb (P3-T4) and 0.5 kb (R-T4) RNAs, which contain *S1025*, had *Rae1*-dependent expression profiles (Fig. 3A and B). The *S1027* probe hybridized to the *Rae1*-sensitive P1-T4 and P3-T4 transcripts, as expected, and to three additional *Rae1*-insensitive species of ~ 1.9 kb, ~ 220 nts and ~ 260 nts (Fig. 3A, middle panel and Fig. 3B). These additional bands were not detected with the *yrzI* and *S1024* probes and their sizes are consistent with transcripts originating at P1 and P3 and terminating at T2 or T3, *i.e.* P1-T2, P1-T3 (indistinguishable in size on the Northern blot) and P3-T2 and P3-T3, respectively (Fig. 3A). The *S1024* probe hybridized to same three major transcripts as the *yrzI* probe (Fig. 3A, right panel). We also detected a very weak additional minor *Rae1*-independent species (around ~ 350 nts), whose origin remains unclear. We did not find any evidence for the use of the putative P2, P4 or P5 promoters under the rich medium conditions tested. More importantly, the most abundant (0.5 kb) species in the *rae1* deleted strain, R-T4, lacks an obvious promoter. We therefore concluded that it most likely results from processing of a primary transcript originating from P1 or P3.

The R-T4 species results from 5' degradation by RNase J1 and is degraded via two alternative pathways

To determine the maturation event(s) that led to the production of the R-T4 species and which RNases

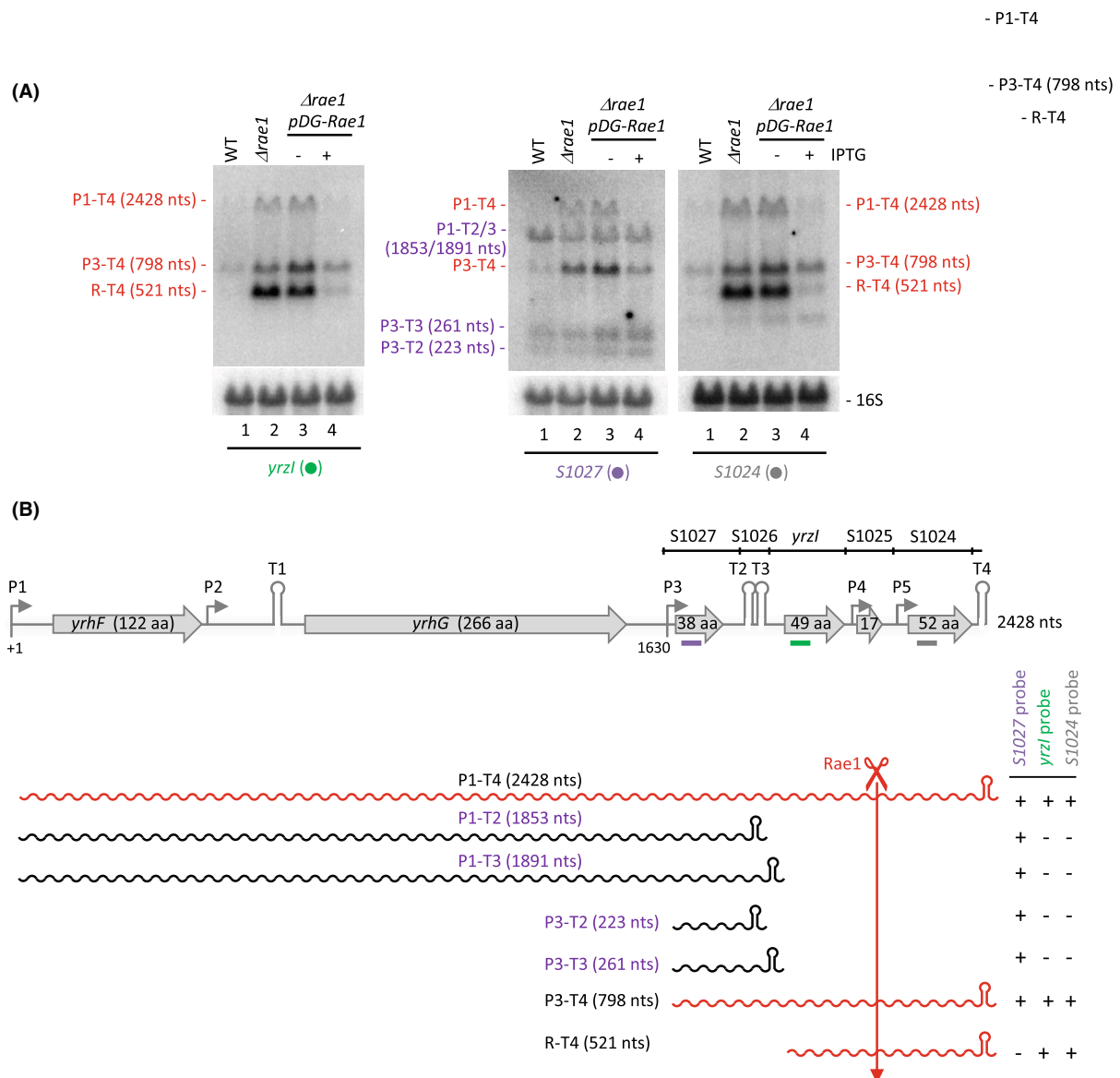


Fig. 3. Mapping of the major RNAs produced from the *yrzI* locus. (A) Northern blots showing expression of the *yrzI* transcript in WT, $\Delta rae1$ and plasmid complemented strains grown in the absence (–) and presence (+) of IPTG. Blots were probed with oligonucleotides complementary to *yrzI* (CC1589; green dot), *S1027* (CC1598; purple dot) and *S1024* (CC1600; gray dot) as indicated. Blots were rehybridized with a probe complementary to 16S rRNA (oligo CC058) as a loading control. This experiment was repeated twice. (B) Structure of the *yrzI* operon and summary of transcripts identified in panel (A). ORFs are represented by gray arrows, the putative promoters by rightward-pointing arrows and putative transcription terminators by the hairpin structures. The sizes of the ORFs are given in amino acids (aa) and the lengths of the intergenic regions in nucleotides (nts) are indicated. The position of the 3 probes used is indicated by colored bars: purple for *S1027*, green for *yrzI* and gray for *S1024*. Transcripts from this locus are shown as wavy lines and those sensitive to Rae1 are in red. The presence or absence of the different species in the Northern blots shown in panel A is represented by (+) or (–) signs, respectively.

eliminate the cleavage products, we performed high-resolution Northern blot analysis in different *B. subtilis* RNase mutants, containing or lacking Rae1.

In the absence of the 5'-exoribonuclease RNase J1 ($\Delta rnfA$), the P3-T4 primary transcript was still detected

but the R-T4 band was replaced by a band migrating about 100 nts slower (referred as E1-T4), detected with both the *yrzI* and *S1024* probes (Fig. 4A, lanes 3 and 11). This suggests that the R-T4 species is generated by RNase J1-mediated degradation from an upstream

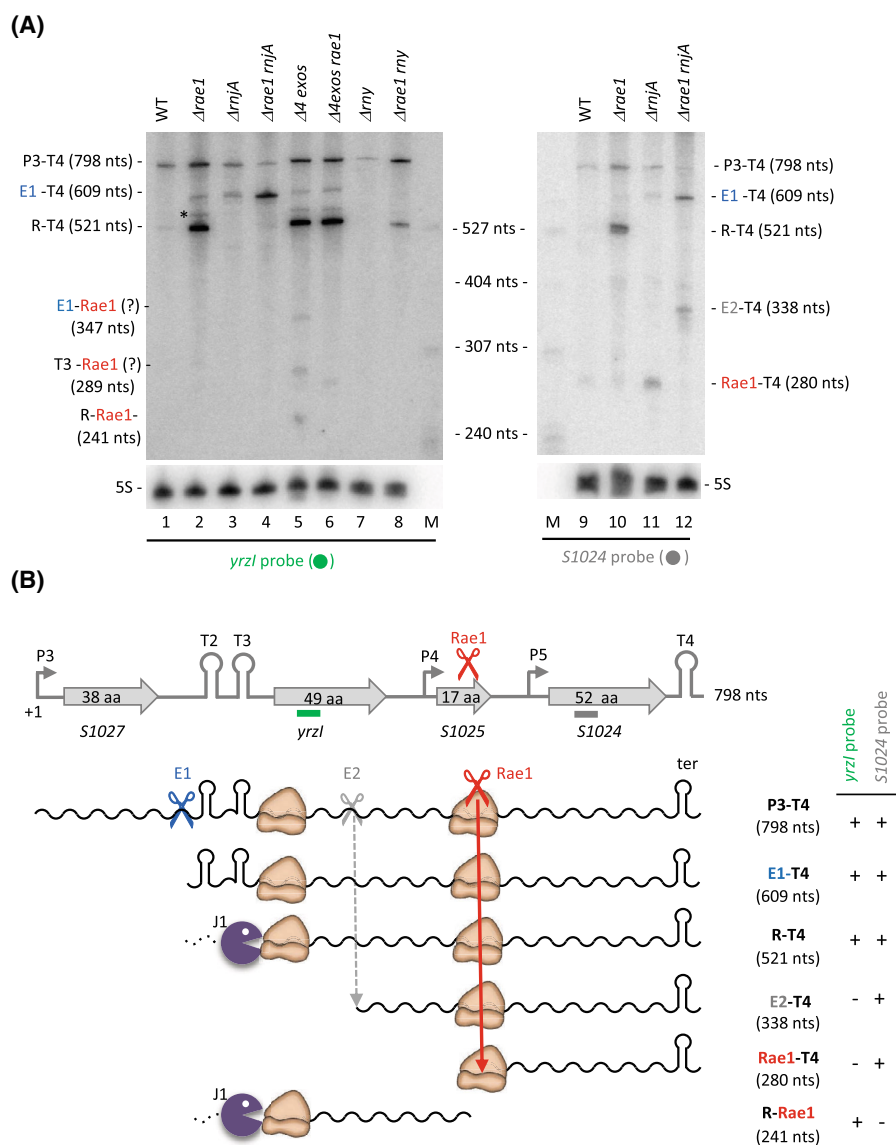


Fig. 4. The R-T4 species results from 5' degradation by RNase J1 is degraded via two alternative pathways (A) Expression of *yrzI* in different RNase mutants. High-resolution Northern blot, probed with oligo CC1589 (*yrzI*; green dot) or CC1600 (*S1024*; gray dot), showing expression of *yrzI* in strains lacking specific *B. subtilis* RNases. Gene abbreviations are as follows: *Rae1* (*rae1*), the four 3'-exoribonucleases PNPase, RNase R, RNase PH and YhaM (*4exos*), RNase J1 (*rnjA*), RNase Y (*rny*). Blots were rehybridized with a probe complementary to 5S rRNA (oligo HP246) as a loading control. The size of the RNAs detected was determined using compilation of 5' end mapping experiments from this study and previous papers [10]. This experiment was repeated twice. (B) Summary of degradation pathways of short *yrzI* operon mRNAs. The structure of the region between *S1027* and *S1024* is shown. ORFs are represented by gray arrows, putative promoters by rightward-pointing arrows and transcription terminators by the hairpin structures. The sizes of the ORFs are given in amino acids (aa) and the positions of probes used are indicated by green and gray bars. The primary transcript (P3-T4) and the degradation intermediates are depicted. Endoribonucleases are symbolized by scissors and exoribonucleases by a Pacman symbol. Ribosomes protecting the 5' end of the R-T4 transcript and involved in *Rae1* cleavage are indicated.

entry site, E1, until RNase J1 reaches the site labeled R (Fig. 4B). The E1-T4 species was more clearly visible in the *Δrae1 rnjA* double mutant strain, consistent with the ability of *Rae1* to trigger its degradation (Fig. 4A, lanes 4 and 12). A weak band (indicated with

an asterisk) that migrates just above the R-T4 species was also detected in the absence of the RNase J1, which may result from inhibition of 5' exoribonucleolytic degradation by RNase J1 at the T2 or T3 terminator hairpins and thus, may correspond to T2-T4 or

T3-T4. This species as well as the R-T4, P3-T4, and E1-T4 RNA were each detected using a probe that hybridized to the T4 terminator confirming they all retain this structure at their 3' ends (Fig. S1).

We addressed the possibility that the major endoribonuclease RNase Y was responsible for the cleavage at E1, by asking whether the E1-T4 and of the R-T4 species were still detectable in the Δrny *raeI* double mutant strain (Fig. 4A, lane 8 and data not shown). The level of R-T4 species was weaker in the Δrny *raeI* strain compared to the $\Delta raeI$ mutant alone and the E1-T4 RNA was no longer detected (Fig. 4A, compare lanes 2 and 8). This suggests that RNase Y contributes to the cleavage at E1 and that either a second endoribonuclease is involved or, in the absence of cleavage by E1 RNase Y, RNase J1 can gain access to the mRNA from a dephosphorylated 5'-end of the primary transcript to generate R-T4.

Strikingly, the R-T4 RNA also strongly accumulated in a $\Delta 4exos$ strain, lacking the four known *B. subtilis* 3'-exoribonucleases (PNPase, RNase PH, RNase R and YhaM) but still expressing Rael (Fig. 4A, compare lane 5 to lane 1), suggesting that R-T4 can also be directly degraded from its 3'-end, independently of Rael. This is unusual as 3'-terminator structures are not typically thought to be vulnerable to direct attack by 3'-exoribonucleases in bacteria [5,23–26]. Three shorter species were additionally detected in the $\Delta 4exos$ strain with the *yrzI* probe, all of which disappeared upon further deleting the *raeI* gene, indicating that they are all dependent on Rael cleavage and contain the S1025 ORF (Fig. 4A, lane 6). The shortest one likely corresponds to the upstream fragment resulting from Rael cleavage of R-T4 (labeled R-Rael in Fig. 4A, lane 5) consistent with the predicted size (241 nts) (Fig. 4B), while the two others could correspond to E1-Rael (347 nts) and T3-Rael (289 nts) respectively. As mentioned above, we suspect that the T3-Rael species results from an inhibition of 5' exoribonucleolytic degradation by RNase J1 by the hairpin of the T3 terminator structure. In the $\Delta 4exos$ *raeI* strain, an additional degradation intermediate of ~270 nts was detected whose origin also remains unclear (Fig. 4A, lane 6).

The use of a probe complementary to S1024 permitted the detection of the ~280-nt downstream cleavage product of the R-T4 species by Rael (Rael-T4) in the *ArnjA* mutant strain but not in the $\Delta raeI$ *rnjA* strain, as expected (Fig. 4A, compare lanes 11 and 12; Fig. 4B). The upstream and downstream fragments resulting from Rael cleavage were also detected in the $\Delta 4exos$ and *rnjA* strains, respectively, in a global study to map sites of endoribonucleolytic cleavage to single

nt resolution [27]. A longer species, which we call E2-T4 (~330 nts) (Fig. 4B), was also detected in the $\Delta raeI$ *rnjA* strain (Fig. 4A, lane 12). As for the R-T4 species, we confirmed that the E2-T4 species possessed the T4 terminator using the T4 probe (Fig. S1, lane 12). The 5'-end of the E2-T4 species corresponds to an additional entry site (E2) for RNase J1, previously mapped by primer extension assay to within the *yrzI* ORF [10]. The endoribonuclease responsible for the cleavage at E2 remains unknown.

Globally, these data indicate that the primary transcripts originating from P1 or P3 are cleaved at the E1 site, followed by 5'-trimming by RNase J1 until it reaches the site labeled R to generate the stable intermediate R-T4. This intermediate can be degraded by either of two pathways: the first is initiated by Rael cleavage, followed by degradation of the products by 5'- and 3'-exoribonucleases, and the second is mediated by 3'-exoribonucleases from the 3'-extremity, independently of Rael. A summary of the RNA processing/degradation pathways for the different RNAs of the *yrzI* operon, combining data from this and our previous paper [10] is shown in Fig. 4B.

The R-T4 species is protected from RNase J1 degradation by ribosomes initiating translation of *yrzI*

The *yrzI* ORF has an exceptionally strong Shine-Dalgarno (SD) sequence, with 11 out of 12 possible Watson-Crick (WC) base pairs with the 3' end of 16S rRNA (Fig. 5A). We therefore postulated that the 5'-end of the R-T4 RNA might result from the blocking of RNase J1 by ribosomes tightly bound to the *yrzI* SD sequence, similar to the phenomenon reported for the *hbs* mRNA in *B. subtilis* and the *cryIIIA* mRNA from *B. thuringiensis* expressed in *B. subtilis*, which possess exceptionally strong SD, or SD-like sequences, respectively [28–31]. The hall-mark of these mRNAs that are protected from RNase J1 degradation is a ribosome 'heel-print' that occurs 8 nts upstream of the first G-residue of the consensus GGAGG SD sequence (Daou-Chabo *et al.*, 2009) (Fig. 5A).

To identify the precise 5'-ends of the main *yrzI* RNAs in *rnjA*⁺ versus *rnjA*⁻ cells, we performed primer extension analysis on total RNA isolated from WT, $\Delta raeI$, $\Delta rnjA$, and $\Delta raeI$ *rnjA* double mutant strains, using a primer hybridizing to *yrzI*. In all four strains, we detected a 5'-end corresponding to the predicted P3 promoter upstream of S1027 (Fig. 5B). The calculated size of the fragment extending from P3 to the terminator following S1024 is 798 nts,

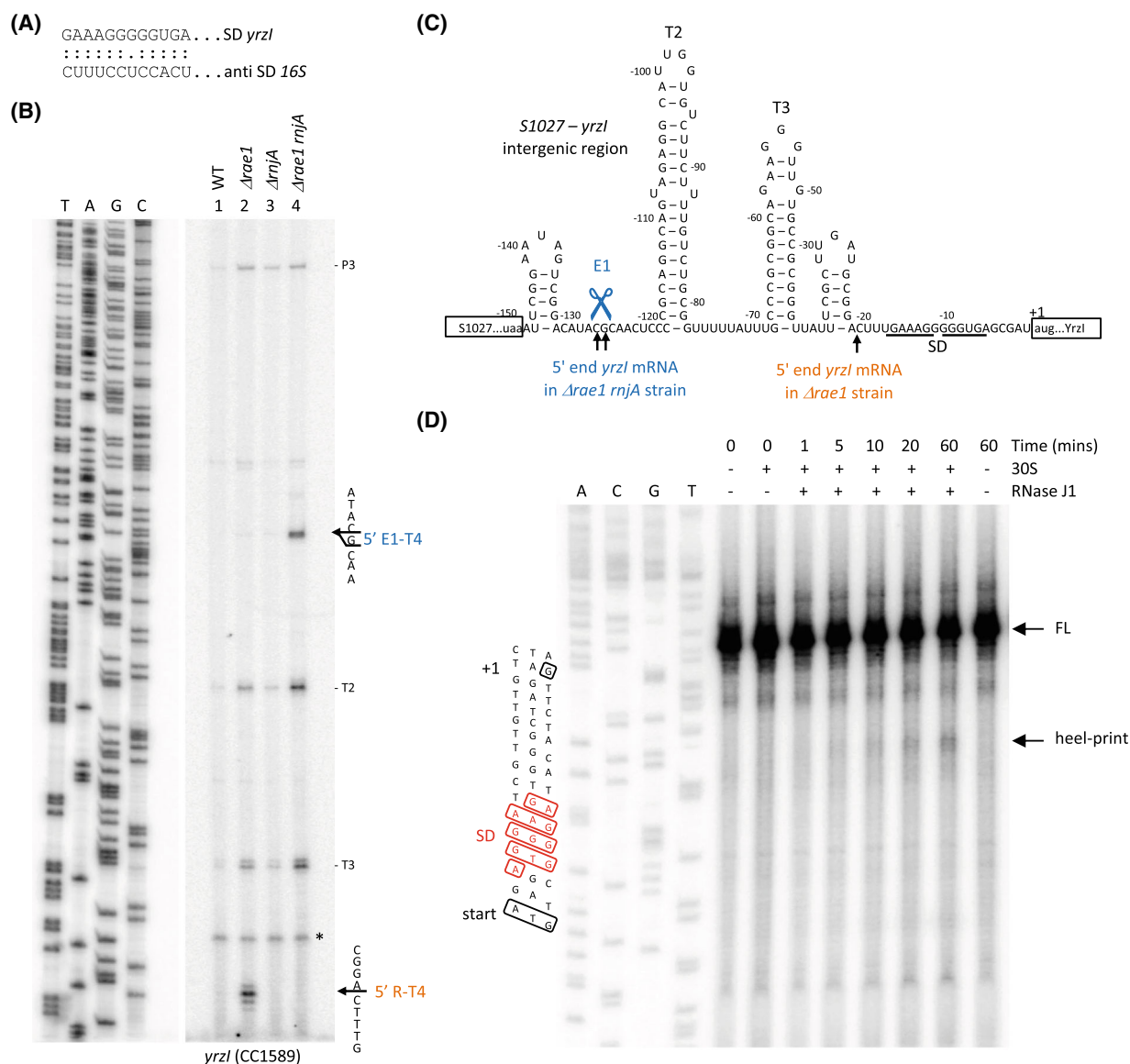


Fig. 5. The 5' end of the R-T4 RNA is protected by a ribosome bound to the *yrzI* SD sequence (A) Potential base pairing between the *yrzI* SD sequence and the 3' end of 16S rRNA. (B) Primer extension assay (oligo CC1589) on total RNA isolated from wild-type (WT) and strains lacking *Rae1* ($\Delta rae1$), RNase J1 ($\Delta rnjA$) and both ($\Delta rae1 rnjA$). Sequence lanes are labeled as their reverse complement to facilitate direct read-out. Mapped 5' ends are shown to the right of the autoradiogram. Reverse transcriptase (RT) stops corresponding to the T2 and T3 terminator structures and the predicted P3 promoter are also indicated. The origin of the band indicated by an asterisk remains unknown. This experiment was repeated twice. (C) Mapping of RNase J1 and *Rae1*-dependent 5' ends to the predicted secondary structure (RNAfold; <http://rna.tbi.univie.ac.at/cgi-bin/RNAWebSuite/RNAfold.cgi>) of the *S1027-yrzI* intergenic region. Co-ordinates are given relative to the AUG start codon of *YrzI* (boxed). The predicted T2 and T3 terminator stem loops are shown. Nucleotides complementary to the anti-Shine Dalgarno sequence of *B. subtilis* 16S rRNA are underlined (SD). (D) Protection by 30S ribosomes against RNase J1 degradation of the *yrzI* transcript. The autoradiogram shows a heel-print assay on a 3'-labeled (p³²Cp) RNA fragment of the *yrzI* transcript in the presence or absence of 30S ribosomes, incubated with RNase J1 for various times. A sequencing reaction on the template DNA was loaded on the left of the gel and labeled as reverse complement to facilitate direct read-out. Note: there is a slight difference in migration (equivalent to about 5 nts for the full-length (FL) transcript and about 4 nts for the heel-print) between the DNA sequence and the RNA reactions due to the 16 Da difference in MW between DNA and RNA nts. This experiment was repeated twice.

corresponding well to the 0.8 kb fragment seen on Northern blots. In $\Delta raeI$ cells, a 5'-end mapping to nt -21 relative to the *yrzI* start codon was strongly visible compared to WT cells (Fig. 5B). This 5' end was located precisely 8 nts upstream of the G-rich motif in the *yrzI* SD sequence (Fig. 5A,C), identical what was observed for the *hbs* and *cryIIIA* ribosome heel-prints [30,31]. The predicted size of a RNA extending from this position to the transcription terminator downstream of *S1024* (T4) is 521 nts and correlates well with the size of the R-T4 band seen on Northern blots. In the $\Delta raeI$ *rnjA* double mutant, the 5' end at nt -21 was no longer visible and was replaced by a species mapping to position -125/126, corresponding to the E1 site (Fig. 4A).

To show that the R-T4 species results from direct ribosome protection of the 521 nt *yrzI* RNA from RNase J1 activity, we transcribed a portion of the *yrzI* gene (-55 to +80 relative to the start codon) using T7 RNA polymerase. The RNA was 3'-labeled with ^{32}P -pCp, pre-incubated with 30S ribosomal subunits and then subjected to RNase J1 degradation *in vitro* for different times. A protected species of the expected size accumulated over time in samples containing 30S subunits (Fig. 5D), confirming that the 5' end of the 521 nt *yrzI* species is protected from RNase J1 degradation by ribosomes initiating translation of the *yrzI* ORF.

Altogether, these data indicate that RNase J1 gains access to the *yrzI* RNAs at the upstream E1 site and degrades until it is blocked by a ribosome bound to the *yrzI* SD at nt -21, giving rise to the R-T4 species.

Degradation of the *yrzI* polycistronic mRNA by 3'-5' exoribonucleases

The data presented above showed that the highly stable R-T4 species can be degraded from its 3' end independently of Rael. We therefore analyzed the ability of individual 3'-exoribonucleases to promote R-T4 degradation by analyzing the profile of *yrzI* RNAs in strains deleted for one or more 3'-exoribonucleases (Fig. 6A). The R-T4 species was present at a higher level in the $\Delta raeI$ $\Delta 4exos$ strain compared to the $\Delta raeI$ strain alone, suggesting that the two degradation pathways involving either Rael or the 3' exoribonucleases, destabilize R-T4 independently (Fig. 6A compare lane 2 and 4). The R-T4 species was not detected in triple mutant $\Delta yhaM$ *rph* *rnr* that only retains PNPase (Fig. 6A, compare lane 7 with lane 5), but was observed in all strains lacking PNPase, albeit at a lower level than in the $\Delta 4exos$ strain (Fig. 6A, compare lanes 6–10 with lane 5). Thus, PNPase appears to

be the major, but not the only 3'-exoribonuclease involved in the degradation of R-T4. A band below P1-T4 (indicated by an asterisk) was also detected in all strains lacking PNPase (Fig. 6A, lanes 5–6 and 8–10). This band may result from exoribonucleolytic degradation mediated by the other 3'-exoribonucleases that are blocked by secondary structure or translating ribosomes. Furthermore, a species migrating slightly faster than the upstream product of Rael cleavage (R-Rael) was additionally observed in all strains lacking PNPase, including the triple mutant Δpnp *rph* *rnr* that only retains YhaM (Fig. 6A, lane 6, white dot). This suggests that YhaM catalyzes the initial shortening of R-Rael and that PNPase is the principal enzyme that finishes the job of degrading it. In contrast, the R-Rael species was only detected in the $\Delta 4exos$ mutants (Fig. 6A, lane 5).

Lastly, we examined the relative contribution of the Rael cleavage pathway and the 3'-exoribonuclease pathway to R-T4 degradation by measuring its stability after addition of rifampicin to the culture medium in the $\Delta raeI$ and $\Delta 4exos$ mutants (Fig. 6B). The R-T4 RNA had a half-life of around 13.5 min in the $\Delta 4exos$ strain, but >18 min in either the $\Delta raeI$ strain or the $\Delta raeI$ $\Delta 4exos$ quintuple mutant, suggesting that the greater contribution comes from the Rael pathway (Fig. 6B). The fact that the half-life of the R-T4 RNA increases in the $\Delta 4exos$ strain compared to WT, despite the presence of Rael, confirms that the effect of the deletion of the four exoribonucleases is at the post-transcriptional level and this 3'-degradation pathway can indeed attack the 3' end of the mRNA independently of Rael (Fig. 6C).

The degradation of R-T4 is thus promoted by two independent rate-limiting degradation pathways one promoted by a translation-dependent cleavage mediated by Rael within S1025 and the other by 3'-exoribonucleases from the 3' end of the mRNA. We postulate that translated R-T4 mRNAs are efficiently degraded by Rael but protected by ribosomes from the 3'-degradation pathway, while untranslated R-T4 mRNAs, which cannot be cleaved by Rael, can be degraded by 3'-exoribonucleases.

Discussion

In this paper, we attribute functions to two of the four peptides encoded by the polycistronic *yrzI* mRNA from *B. subtilis*: the short 49-aa inhibitory peptide, called YrzI, and its antidote, a 17-aa peptide called S1025. We propose to rename YrzI and S1025 as SpyT and SpyA for Small peptide YrzI Toxin and Small peptide YrzI Antitoxin, respectively. We also describe

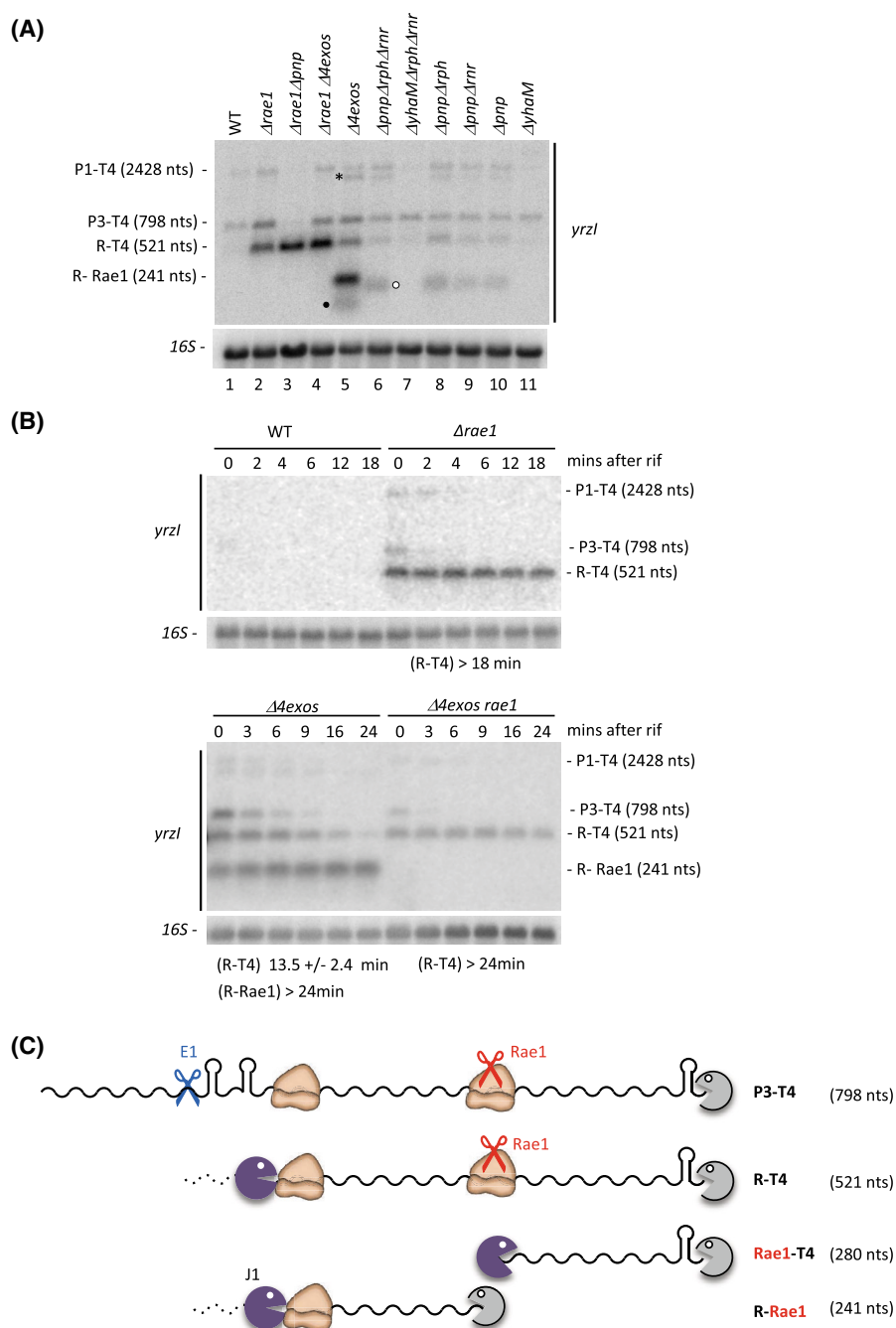


Fig. 6. Degradation of the *yrzI* polycistronic mRNA by 3'-5' exoribonucleases. (A) Northern blot, probed with oligo CC1589 (*yrzI*), showing expression of *yrzI* in strains lacking specific *B. subtilis* RNases. Gene abbreviations are as follows: Rae1 (*rae1*), the four 3'-exoribonucleases PNPase, RNase R, RNase PH and YhaM (*4exos*), PNPase (*pnp*), RNase PH (*rph*), RNase R (*mr*) and YhaM (*yhaM*). The origin of the band indicated by a black dot blot remains unknown. This experiment was repeated twice. (B) Half-lives were determined by Northern blot analysis in WT, Δ *rae1*, Δ *4exos* and Δ *rae1* Δ *4exos* strains at mid-log phase in rich medium at times after rifampicin addition, probed with oligo CC1589 (*yrzI*). Blots in panels A and B were rehybridized with a probe complementary to 16S rRNA (oligo CC058) as a loading control. Note that the measured half-life of the R-Rae1 is impacted by the fact that it is being continually generated by processing of P3-T4 as it is being decayed. This experiment was repeated twice. (C) Degradation pathways of R-T4 RNA. The primary transcript (P3-T4) and the degradation intermediates are depicted. Endoribonucleases are symbolized by scissors and exoribonucleases by a Pacman symbol.

a second naturally occurring case in *B. subtilis* of a ribosome bound to an exceptionally strong SD sequence protecting an mRNA fragment from 5'-degradation by RNase J1 (the other example being *hbs*) [29–31]. We further describe the non-canonical degradation pathways required to eliminate this species involving the translation-dependent endoribonuclease Rae1, on the one hand, and direct attack from the 3'-end by exoribonucleases on the other.

The SpyT toxin peptide is highly conserved among the genus *Bacillus* (Fig. S2A,B). A sequence encoding a peptide highly homologous to the SpyA antitoxin was identified downstream of the *spyT* ORF in all analyzed *Bacillus* genomes, except for *B. cereus* (Fig. S2A,B). In *B. cereus*, SpyT peptides that exhibit lower homology to SpyT from *B. subtilis* are present in seven contiguous copies, but the ORF located immediately downstream does not share significant homology with the *B. subtilis* SpyA peptide (Fig. S2C). Although the *spyTA* operon is expressed most of the time in *B. subtilis*, pointing to a general role in the cell's physiology, it shows peaks of expression in the cold, in stationary phase and late in sporulation [22], suggesting it may have specific functions under these conditions.

There are some intriguing parallels between the SpyT/SpyA/Rae1 triad and classical toxin-antitoxin (TA) systems. As currently observed in TA modules, the SpyT toxin and SpyA antitoxin are encoded within the same operon. TA modules have been divided into seven classes according to the mode of action of the antitoxin [32–34]. We had previously identified a type II TA system in *B. subtilis*: the toxin EndoA (an RNase member of the MazF/PemK family of bacterial toxins) and the YdcD antitoxin protein encoded by the gene immediately upstream [35]. Our data suggest that SpyT/SpyA/Rae1 triad could potentially constitute a toxin/double-antitoxin system, with components resembling both the type II (protein antitoxin) and type V (RNase antitoxin) TA systems. On one hand, protection by SpyA against the toxic effect of SpyT was observed even in the absence of Rae1 indicating that the SpyA peptide is the major antidote to the SpyT toxin. On the other hand, Rae1 could easily counteract SpyT toxicity by promoting the degradation of the toxin-antitoxin mRNA, if SpyA peptide levels were insufficient to fully neutralize SpyT. Clearly, Rae1 does not serve as an antitoxin in cells growing in rich medium as a Δ *rae1* strain has no major phenotype under these conditions. However, we cannot exclude that there may be certain growth conditions where expression of SpyT and SpyA become uncoupled and SpyA levels are insufficient to do the job alone. In this case, the double protection afforded by Rae1 could be beneficial. A parallel can be

drawn with the RatA/TxpA and YonT/as YonT type I TA systems of *B. subtilis* where the toxin-encoding mRNAs are degraded by RNase III [36]. However, in those cases inactivation of RNase III in rich medium is lethal.

Our data indicate that the *spyTA* and *bmrBCD* operons are both governed at the transcriptional level by AbrB and at the post-transcriptional level by Rae1 [12], suggesting there may be some as yet uncovered link between the two. Post-transcriptional modulation of *spyT* expression first involves stabilization of the R-T4 fragment through cleavage by an endoribonuclease at the E1 site followed by 5'-trimming by RNase J1 until it is blocked by a ribosome bound at the SD sequence of *spyT*. The stabilized mRNA is then principally degraded through translation-dependent cleavage by Rae1. About 200 genes are predicted to have exceptionally strong SD sequences less than 20 nts upstream of their ORFs in *B. subtilis*, with maximum 2 mismatches out of 12 with the 3'-end of 16S rRNA equivalent to the experimentally confirmed *hbs* gene. Thus, at a conservative estimate at least 5% of *B. subtilis* genes are predicted to benefit from 5'-protection by ribosomes initiating translation at their SD sequences (Table S3). Note, however, that the original stabilizing motif in the *B. thuringiensis cryIIIA* mRNA (Stab SD) expressed in *B. subtilis* had only 8/12 consecutive base pairs [37] and so the actual number of mRNAs falling into this category may be much higher.

The *spyTA* polycistronic mRNA is targeted by several RNases: two endoribonucleolytic sites (E1 and E2) were mapped in addition to the Rae1 cleavage site. Our data suggest that RNase Y may cleave at E1, but further investigation is needed to determine whether other RNases also participate and to identify the RNase responsible for E2 cleavage. Remarkably, 3'-exoribonucleases can also participate in the degradation of the mature R-T4 RNA, despite the presence of the hairpin structure of the transcriptional terminator T4 at its 3' end. Although Rho-independent transcription terminators are often described as providing resistance against 3' degradation by exoribonucleases [5,23–26], the phenomenon has been understudied in bacteria and is likely to be dependent on the intrinsic stability of the RNA hairpins and/or additional factors. Indeed, the predicted stability of the transcription terminator at the end of the *spyTA* operon is 11.1 kcal·mol⁻¹, well below the average stability of experimentally determined Rho-independent terminators in *B. subtilis* of 16 kcal·mol⁻¹ [38]. This may explain why the 3'-degradation pathway comes into play for this particular mRNA that is protected by ribosomes at the 5' end from the RNase J1. Although

the R-T4 RNA was strongly stabilized in the $\Delta 4exos$ mutant, it showed no signs of decay over the time-course of the experiment in strains lacking Rael. This unusual scenario, in which two rate-limiting degradation pathways target the same mRNA, can be explained by hypothesizing that translated *spyTA* operon mRNAs are efficiently degraded by Rael, while untranslated *spyTA* mRNAs, which cannot be cleaved by Rael, are eliminated by 3'-exoribonucleases.

This study of the *spyTA* polycistronic mRNA turnover highlights the complex interplay between ribosomes and the mRNA degradation machinery: degradation of the most abundant mRNA R-T4 species, generated by ribosomes obstructing 5'-exoribonucleolytic degradation, is influenced by the translational status of the mRNA for Rael-dependent cleavage and likely also for the 3'-exoribonuclease pathway.

Acknowledgements

We thank lab members for helpful discussion. This work was supported by funds from the CNRS and Université Paris Cité (UMR8261), the Agence Nationale de la Recherche (ARNr-BasRael), Labex Dynamo and Equipex Cacsice).

Author contributions

LG and ML contributed equally to the execution of the experiments. AM performed the genomic analyses to predict exceptionally strong SD sequences. CC helped supervise the project and wrote the manuscript. FB performed the experiments, supervised the project and wrote the manuscript.

Peer review

The peer review history for this article is available at <https://www.webofscience.com/api/gateway/wos/peer-review/10.1002/1873-3468.70027>.

Data availability

The data that support the findings of this study are available from the corresponding author on request.

References

- 1 Bechhofer DH and Deutscher MP (2019) Bacterial ribonucleases and their roles in RNA metabolism. *Crit Rev Biochem Mol Biol* **54**, 242–300.
- 2 Trinquier A, Durand S, Braun F and Condon C (2020) Regulation of RNA processing and degradation in bacteria. *Biochim Biophys Acta Gene Regul Mech* **1863**, 194505.
- 3 Richards J, Liu Q, Pellegrini O, Celesnik H, Yao S, Bechhofer DH, Condon C and Belasco JG (2011) An RNA pyrophosphohydrolase triggers 5'-exonucleolytic degradation of mRNA in *Bacillus subtilis*. *Mol Cell* **43**, 940–949.
- 4 Durand S, Gilet L, Bessieres P, Nicolas P and Condon C (2012) Three essential ribonucleases-RNase Y, J1, and III-control the abundance of a majority of *Bacillus subtilis* mRNAs. *PLoS Genet* **8**, e1002520.
- 5 Braun F, Le Derout J and Regnier P (1998) Ribosomes inhibit an RNase E cleavage which induces the decay of the rpsO mRNA of *Escherichia coli*. *EMBO J* **17**, 4790–4797.
- 6 Deana A and Belasco JG (2005) Lost in translation: the influence of ribosomes on bacterial mRNA decay. *Genes Dev* **19**, 2526–2533.
- 7 Dreyfus M (2009) Killer and protective ribosomes. *Prog Mol Biol Transl Sci* **85**, 423–466. doi: [10.1016/S0079-6603\(08\)00811-8](https://doi.org/10.1016/S0079-6603(08)00811-8)
- 8 Duviau MP, Chen F, Emile A, Coccagn-Bousquet M, Girbal L and Nouaille S (2023) When translation elongation is impaired, the mRNA is uniformly destabilized by the RNA degradosome, while the concentration of mRNA is altered along the molecule. *Nucleic Acids Res* **51**, 2877–2890.
- 9 Iost I and Dreyfus M (1995) The stability of *Escherichia coli* lacZ mRNA depends upon the simultaneity of its synthesis and translation. *EMBO J* **14**, 3252–3261.
- 10 Leroy M, Piton J, Gilet L, Pellegrini O, Proux C, Coppee JY, Figaro S and Condon C (2017) Rael/YacP, a new endoribonuclease involved in ribosome-dependent mRNA decay in *Bacillus subtilis*. *EMBO J* **36**, 1167–1181.
- 11 Condon C, Piton J and Braun F (2018) Distribution of the ribosome associated endonuclease Rael and the potential role of conserved amino acids in codon recognition. *RNA Biol* **15**, 1–6.
- 12 Deves V, Trinquier A, Gilet L, Alharake J, Condon C and Braun F (2023) Shutdown of multidrug transporter bmrCD mRNA expression mediated by the ribosome-associated endoribonuclease (Rael) cleavage in a new cryptic ORF. *RNA* **29**, 1108–1116.
- 13 Li GW, Oh E and Weissman JS (2012) The anti-Shine-Dalgarno sequence drives translational pausing and codon choice in bacteria. *Nature* **484**, 538–541.
- 14 Oussenko IA, Abe T, Ujiiie H, Muto A and Bechhofer DH (2005) Participation of 3'-to-5' exoribonucleases in the turnover of *Bacillus subtilis* mRNA. *J Bacteriol* **187**, 2758–2767.

- 15 Bechhofer DH, Oussenko IA, Deikus G, Yao S, Mathy N and Condon C (2008) Analysis of mRNA decay in *Bacillus subtilis*. *Methods Enzymol* **447**, 259–276.
- 16 Stead MB, Agrawal A, Bowden KE, Nasir R, Mohanty BK, Meagher RB and Kushner SR (2012) RNAsnap: a rapid, quantitative and inexpensive, method for isolating total RNA from bacteria. *Nucleic Acids Res* **40**, e156.
- 17 Britton RA, Wen T, Schaefer L, Pellegrini O, Uicker WC, Mathy N, Tobin C, Daou R, Szyk J and Condon C (2007) Maturation of the 5' end of *Bacillus subtilis* 16S rRNA by the essential ribonuclease YkqC/RNase J1. *Mol Microbiol* **63**, 127–138.
- 18 Jurenas D, Fraikin N, Goormaghtigh F and Van Melderen L (2022) Biology and evolution of bacterial toxin-antitoxin systems. *Nat Rev Microbiol* **20**, 335–350.
- 19 Reilman E, Mars RA, van Dijl JM and Denham EL (2014) The multidrug ABC transporter BmrC/BmrD of *Bacillus subtilis* is regulated via a ribosome-mediated transcriptional attenuation mechanism. *Nucleic Acids Res* **42**, 11393–11407.
- 20 Chumsakul O, Takahashi H, Oshima T, Hishimoto T, Kanaya S, Ogasawara N and Ishikawa S (2011) Genome-wide binding profiles of the *Bacillus subtilis* transition state regulator AbrB and its homolog Abh reveals their interactive role in transcriptional regulation. *Nucleic Acids Res* **39**, 414–428.
- 21 Chumsakul O, Nakamura K, Kurata T, Sakamoto T, Hobman JL, Ogasawara N, Oshima T and Ishikawa S (2013) High-resolution mapping of in vivo genomic transcription factor binding sites using in situ DNase I footprinting and ChIP-seq. *DNA Res* **20**, 325–338.
- 22 Nicolas P, Mader U, Dervyn E, Rochat T, Leduc A, Pigeonneau N, Bidnenko E, Marchadier E, Hoebeke M, Aymerich S *et al.* (2012) Condition-dependent transcriptome reveals high-level regulatory architecture in *Bacillus subtilis*. *Science* **335**, 1103–1106.
- 23 Deikus G and Bechhofer DH (2007) Initiation of decay of *Bacillus subtilis* trp leader RNA. *J Biol Chem* **282**, 20238–20244.
- 24 Farr GA, Oussenko IA and Bechhofer DH (1999) Protection against 3'-to-5' RNA decay in *Bacillus subtilis*. *J Bacteriol* **181**, 7323–7330.
- 25 Lecrivain AL, Le Rhun A, Renault TT, Ahmed-Begriff R, Hahnke K and Charpentier E (2018) In vivo 3'-to-5' exoribonuclease targetomes of streptococcus pyogenes. *Proc Natl Acad Sci USA* **115**, 11814–11819.
- 26 Spickler C and Mackie GA (2000) Action of RNase II and polynucleotide phosphorylase against RNAs containing stem-loops of defined structure. *J Bacteriol* **182**, 2422–2427.
- 27 Taggart JC, Dierksheide J, Leblanc H, Lalanne JB, Durand S, Braun F, Condon C and Li GW (2024) A high-resolution view of RNA endonuclease cleavage in *Bacillus subtilis*. *bioRxiv* **10.1101/2023.03.12.532304** [PREPRINT]
- 28 Agaisse H and Lereclus D (1996) STAB-SD: a Shine-Dalgarno sequence in the 5' untranslated region is a determinant of mRNA stability. *Mol Microbiol* **20**, 633–643.
- 29 Braun F, Durand S and Condon C (2017) Initiating ribosomes and a 5'/3'-UTR interaction control ribonuclease action to tightly couple *B. Subtilis* hbs mRNA stability with translation. *Nucleic Acids Res* **45**, 11386–11400.
- 30 Daou-Chabo R, Mathy N, Benard L and Condon C (2009) Ribosomes initiating translation of the hbs mRNA protect it from 5'-to-3' exoribonucleolytic degradation by RNase J1. *Mol Microbiol* **71**, 1538–1550.
- 31 Mathy N, Benard L, Pellegrini O, Daou R, Wen T and Condon C (2007) 5'-to-3' exoribonuclease activity in bacteria: role of RNase J1 in rRNA maturation and 5' stability of mRNA. *Cell* **129**, 681–692.
- 32 Aakre CD, Phung TN, Huang D and Laub MT (2013) A bacterial toxin inhibits DNA replication elongation through a direct interaction with the beta sliding clamp. *Mol Cell* **52**, 617–628.
- 33 Goeders N and Van Melderen L (2014) Toxin-antitoxin systems as multilevel interaction systems. *Toxins* **6**, 304–324.
- 34 Wang X, Yao J, Sun YC and Wood TK (2021) Type VII toxin/antitoxin classification system for antitoxins that enzymatically neutralize toxins. *Trends Microbiol* **29**, 388–393.
- 35 Pellegrini O, Mathy N, Gogos A, Shapiro L and Condon C (2005) The *Bacillus subtilis* ydcDE operon encodes an endoribonuclease of the MazF/PemK family and its inhibitor. *Mol Microbiol* **56**, 1139–1148.
- 36 Durand S, Gilet L and Condon C (2012) The essential function of *B. subtilis* RNase III is to silence foreign toxin genes. *PLoS Genet* **8**, e1003181.
- 37 Agaisse H and Lereclus D (1994) Structural and functional analysis of the promoter region involved in full expression of the *cryIIIA* toxin gene of *Bacillus thuringiensis*. *Mol Microbiol* **13**, 97–107.
- 38 de Hoon MJ, Makita Y, Nakai K and Miyano S (2005) Prediction of transcriptional terminators in *Bacillus subtilis* and related species. *PLoS Comput Biol* **1**, e25.
- 39 Karp PD, Billington R, Caspi R, Fulcher CA, Latendresse M, Kothari A, Keseler IM, Krummenacker M, Midford PE, Ong Q *et al.* (2019) The BioCyc collection of microbial genomes and metabolic pathways. *Brief Bioinform* **20**, 1085–1093.
- 40 Sievers F and Higgins DG (2018) Clustal omega for making accurate alignments of many protein sequences. *Protein Sci* **27**, 135–145.

Supporting information

Additional supporting information may be found online in the Supporting Information section at the end of the article.

Fig. S1. Validation of presence of T4 terminator at 3' end of *yrzI* transcripts.

Fig. S2. Conservation of *yrzI* operon in the genus *Bacillus*.

Table S1. Oligonucleotides used in this study.

Table S2. *Bacillus subtilis* strains used in this study.

Table S3. Predicted exceptionally strong SD sequences in *B. subtilis*.